ANALYSIS OF DARK MANTLE DEPOSITS ON THE NORTHEASTERN LIMB OF THE MOON WITH M3, LROC, AND KAGUYA DATA SETS. J.Olaf Gustafson[1] and L.R. Gaddis[2]. [1]Dept. Earth & Atmospheric Sciences, Cornell University, Ithaca, NY; [2]Astrogeology Science Center, U.S. Geological Survey, Flagstaff, AZ. (jg72@cornell.edu).

Introduction: We have examined dark-mantle deposits (DMDs) previously identified on the northeastern limb of the Moon using monochrome and multispectral image data and associated derived products from a variety of recent lunar remote sensing instruments. The NE limb hosts a number of distinct centers of pyroclastic volcanism which have not been thoroughly characterized. Our objective is to assess interdeposit and intradeposit compositional variations among the NE limb DMDs and compare them to other volcanic deposits both within this region and elsewhere across the Moon. These goals support both a volcanological analysis of the origin of these resourse-rich deposits (e.g., FeO, TiO2, Oxygen [1-4]) and a future geologic assessment of those resources.

Background: Numerous pyroclastic deposits have been mapped across the Moon, typically based on their low albedo, smooth texture, and mantling effect over underlying terrain features [5-8]. Gaddis *et al.* [5] compared the composition of 75 potential lunar pyroclastic deposits using Clementine spectral reflectance (CSR) measurements. For this study, we focus on a region along the northeastern limb of the Moon that contains ten DMDs at five locations (***Fig. 1***): Atlas (D=87 km), a floor-fractured crater (FFC) with two DMDs; Franklin (D=56 km), a FFC which contains a patchy DMD and several irregular craters that are possible source vents; Messala (D=127 km), which contains two adjacent DMDs associated with fissures; Gauss (D=178 km), a FFC with three distinct DMD groups; and Mare Frigoris, the eastern portion of which contains two mapped DMDs associated with fissures. The results presented here build on previous studies of the Atlas, Franklin, Gauss, and Frigoris DMDs [8-12].

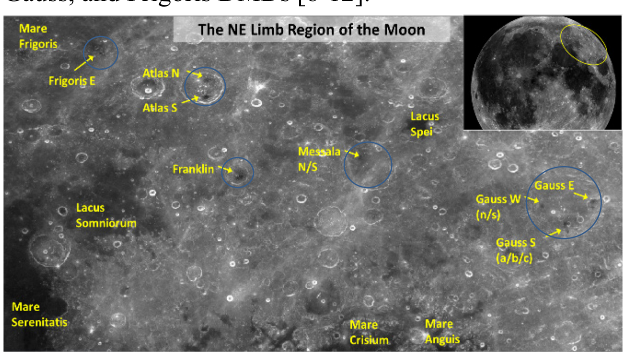

Fig. 1- Study area on the NE limb of the Moon (portion of global WAC mosaic [14], NASA/GSFC/ASU).

Methods: The LRO WAC acquires multispectral images at two ultraviolet (UV) and five visible (VIS) wavelengths at a resolution of ~400 m/pix UV and ~75 m/pix VIS [13,14]. The M3 instrument acquired multispectral images across a spectral range 0.4-3µm at 20 nm spectral resolution, with a spatial resolution of ~140-280m/pix [15]. We used Level 2 data, primarily from Optical Period 2. Our spectral processing followed the procedure described in [16]: smoothing, defining the continuum function using a 3-segment linear convex hull with dynamically chosen tie points for each spectrum, and then calculating the continuum-removed spectrum [17]. Glass abundance estimates were produced following the methods of Horgan *et al.*[18]. The Kaguya Multiband Imager (MI) obtained images in 5 UV-VIS bands and 4 NIR bands. The spatial resolution was about 20 m/pix for the UVVIS bands and 62 m/pix for the four NIR bands [19,20]. In this study, we used derived FeO abundance products based on data from the MAP 02 processing level [21,22] obtained through the ACT-REACT-Quickmap web interface (https://quickmap.lroc.asu.edu).

Results and Discussion: Our initial analysis of the NE limb region using the combined data sets has focused on comparing M3 spectra among all the deposits, along with a more detailed examination of the Franklin DMD to include morphology, spectral parameter maps, and derived mineral and glass abundances. NE limb pyroclastic deposts exhibit a range of spectral reflectance patterns that reveal differences in mineralogy and/or crystallinity (***Fig. 2***). A typical Cpx-rich mare signature is seen in the Frigoris Mare spectrum; the DMDs at Frig-E and Gauss-S are similar but with a 1-µm shoulder and shorter 2-µm center indicative of an additional glassy component. The Gauss-S(a) spectrum is likely influenced by the presence of Cpx in the effusive portion of the deposit adjacent to the mantled region [12]. Franklin and Messala spectra are similar to each other, with shorter band centers and a shallower 1-µm band indicating a mixture of Opx with minor amounts of glass. Atlas-S is similar, but with a much stronger glass component to the spectrum. Finally, Gauss-E has a classic glass-rich spectrum, with a long 1-µm center, short 2-µm center, and a deep 1-µm band shoulder.

Compositional trends are illustrated in the spectral parameter plot (***Fig. 3***); dashed boxes are shown outlining regions identified by [16] as being dominated by Cpx-rich, Opx-rich, or glassy materials, and SE limb volcanic deposit spectral groups identified by [17]. Spectral parameter trends vary within locations in some

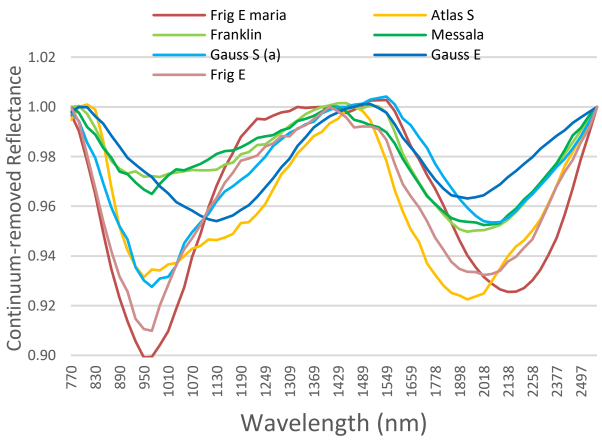

Fig. 2- M3 continuum-removed spectra of selected NE limb DMDs and the Frigoris mare deposit.

cases; for example, the Gauss deposits fall into three groups: Gauss-S(a) being similar to Frig-E, Gauss-S(c) and W(s) being similar to Atlas-N and S, and Gauss-E, W(n), and S(b) forming a distinct high-glass spectral group. This suggests that within Gauss, DMD spectra are likely influenced not only by the mineralogy of the erupted material but also by differences in crystallinity and the ratio of juvenile material to locally derived clastics entrained during the eruption.

Our analysis also incorporates compositional maps created using both M3 spectral parameters and derived FeO concentrations. Here we present examples of these maps for Franklin (***Figs. 4b, 4c***). Preliminary review of the Franklin spectral maps confirms that the often-glassy, mafic mantling material was erupted from vents and fissures which appear as irregular craters in the ref lectance images. These maps also highlight the boundaries of the DMD and reveal patterns in the the density of emplaced material around the vents.

Conclusions and Future Work: Our analysis has identified spectral differences between DMDs hosted at different locations on the NE limb, but we have also found that variations in crystallinity and glass content appear to be a major influence on the DMD spectra across the area. We will extend our analysis to produce spectral parameter and compositional maps of all NE limb DMDs to identify similarities and differences that will help illuminate the volcanic and magmatic history and resource potential of this region.

References: [1] Allen (2015) *LPS 46th* #1140; [2] Allen *et al.* (1996) *JGR 101*, 26085-26095; [3] Coombs *et al.* (1998) *Proc. Space 98*, 608–615; [4] Hawke *et al.* (1990) *LPS 20th*, 249–258; [5] Gaddis *et al*. (2003) *Icarus 161*, 262-280; [6] Head (1974) *PLSC 5th*, 207-222; [7] Gaddis *et al.* (1985) *Icarus 61*, 461-488; [8] Hawke *et al.* (1989) *LPS 19th*, 255-268; [9] Gaddis *et al.* (2012) *LPS 43rd* #2787; [10] Kramer *et al.* (2015) *JGR 120*, 1646-1670; [11] Trang *et al.* (2017) *Icarus 283*, 232–253; [12] Gustafson *et al.* (2017) *LPS 48th* #2605; [13] Robinson *et al.* (2010) *Space Sci. Rev. 150* (1-4), 81-124; [14] Scholten *et al.* (2011) *LPS 42nd* #2046; [15] Pieters *et al.* (2009) *Curr. Sci. 96*(4), 500-505; [16] Bennett *et al.* (2016) *Icarus 273*, 296-314; [17] Gustafson *et al.* (in review), *Icarus*; [18] Horgan *et al.* (2014) *Icarus 234*, 132–154; [19] Haruyama *et al.* (2008) *EPS 60*, 243–255; [20] Ohtake *et al.* (2008) *EPS 60*, 257-264; [21] Lemelin *et al.* (2016) *LPS 47th* #2994; [22] Ohtake *et al.* (2013) *Icarus 226* (1), 364–374.

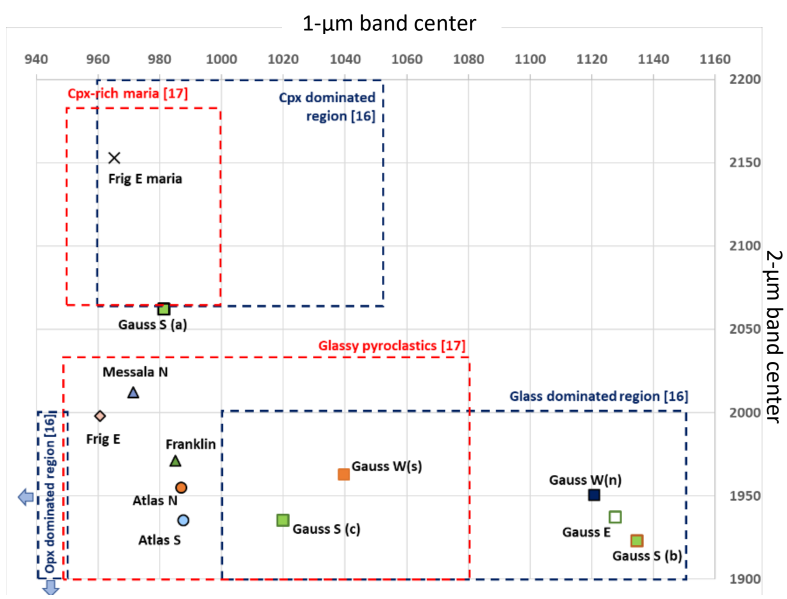

Fig. 3 – plot of 1-µm vs. 2-µm band centers derived from M3 spectra. Colored boxes show compositional regions defined by [16] and [17]. Most NE limb DMDs fall into the "glass dominated' and "glassy pyroclastics" regions.

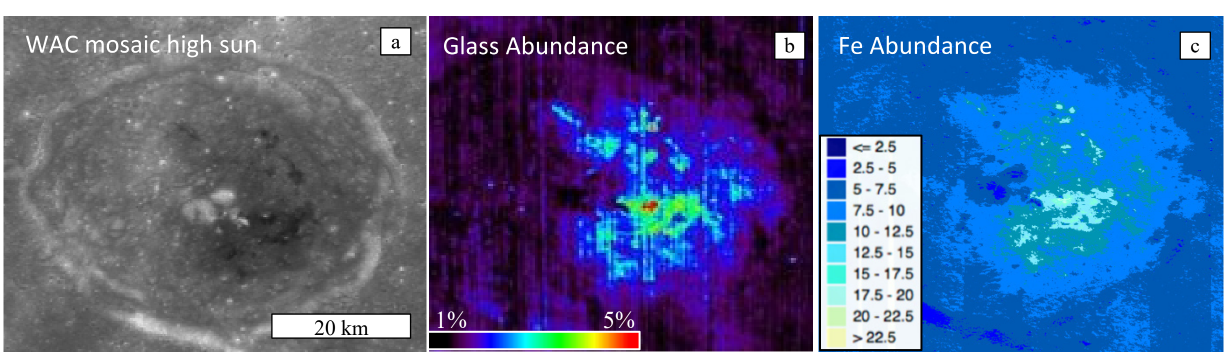

Fig. 4 – Franklin crater showing (a) M3 reflectance at 1489 nm; (b) glass abundance derived from M3 spectra; and (c) Fe abundance derived from MI spectra.